Caveolin-1: a critical regulator of lung fibrosis in idiopathic pulmonary fibrosis

Xiao Mei Wang,[1] Yingze Zhang,[1] Hong Pyo Kim,[1] Zhihong Zhou,[1] Carol A. Feghali-Bostwick,[1] Fang Liu,[1] Emeka Ifedigbo,[1] Xiaohui Xu,[2] Tim D. Oury,[3] Naftali Kaminski,[1] and Augustine M.K. Choi[1]

[1]Division of Pulmonary, Allergy, and Critical Care Medicine, Department of Medicine, University of Pittsburgh, Pittsburgh, PA 15213
[2]Department of Epidemiology, Graduate School of Public Health, University of Pittsburgh, Pittsburgh, PA 15261
[3]Department of Pathology, School of Medicine, University of Pittsburgh, Pittsburgh, PA 15261

Idiopathic pulmonary fibrosis (IPF) is a progressive chronic disorder characterized by activation of fibroblasts and overproduction of extracellular matrix (ECM). Caveolin-1 (cav-1), a principal component of caveolae, has been implicated in the regulation of numerous signaling pathways and biological processes. We observed marked reduction of cav-1 expression in lung tissues and in primary pulmonary fibroblasts from IPF patients compared with controls. We also demonstrated that cav-1 markedly ameliorated bleomycin (BLM)–induced pulmonary fibrosis, as indicated by histological analysis, hydroxyproline content, and immunoblot analysis. Additionally, transforming growth factor β1 (TGF-β1), the well-known profibrotic cytokine, decreased cav-1 expression in human pulmonary fibroblasts. cav-1 was able to suppress TGF-β1–induced ECM production in cultured fibroblasts through the regulation of the c-Jun N-terminal kinase (JNK) pathway. Interestingly, highly activated JNK was detected in IPF- and BLM-instilled lung tissue samples, which was dramatically suppressed by ad–cav-1 infection. Moreover, JNK1-null fibroblasts showed reduced smad signaling cascades, mimicking the effects of cav-1. This study indicates a pivotal role for cav-1 in ECM regulation and suggests a novel therapeutic target for patients with pulmonary fibrosis.

CORRESPONDENCE
Augustine M.K. Choi:
choiam@upmc.edu

Abbreviations used: α-SMA, α–smooth muscle actin; BLM, bleomycin; cav-1, caveolin-1; ECM, extracellular matrix; ERK, extracellular signal–regulated protein kinase; H&E, hematoxylin and eosin; IPF, idiopathic pulmonary fibrosis; JNK, c-Jun N-terminal kinase; MAPK, mitogen-activated protein kinase.

Caveolae are flask-shaped invaginated membrane vesicles with a diameter of 50–100 nm. They are characterized by the existence of a group of 22–24-kD integral membrane proteins termed caveolins. Among the three caveolins identified to date, caveolin-1 (cav-1) is the most extensively characterized and is regarded as the biochemical marker of caveolae in many cell types (1). It forms a high molecular complex and interacts with cav-2 (2). The most abundant cav-1–expressing cells are fibroblasts, endothelial cells, type I pneumocytes, and adipocytes (3). cav-3 expression is restricted to muscle cells (4). Many cellular functions have been attributed to caveolae and cav-1, including membrane trafficking, endocytosis, regulation of calcium homeostasis, lipid metabolism, and signal transduction in cellular proliferation and apoptosis (1). Because of the distinctive lipid composition (rich in glycosphingolipids, sphingomyelin, and cholesterol), caveolae function to concentrate many lipid-attached signal molecules into one specialized membrane organelle. cav-1, the scaffolding protein of caveolae, interacts with many signaling molecules and regulates their activation (5). For example, cav-1 inhibits the activation of growth factor receptors, such as the epidermal growth factor receptor (6) and the platelet-derived growth factor receptor (7), and the downstream mitogen-activated protein kinase (MAPK) and phosphoinositide 3–kinase pathways, resulting in reduced cell growth and increased apoptosis.

Idiopathic pulmonary fibrosis (IPF) is a progressive chronic interstitial lung disease with a high mortality (median survival of newly diagnosed patients is ∼3 yr) and uniformly poor prognosis (8). The pathogenesis of IPF is still poorly understood. Current medical therapies, such as corticosteroids, cytotoxic drugs, and IFN-γ, have been based on attempts to suppress the inflammatory and fibrotic process but have thus far offered little benefit against the

The online version of this article contains supplemental material.

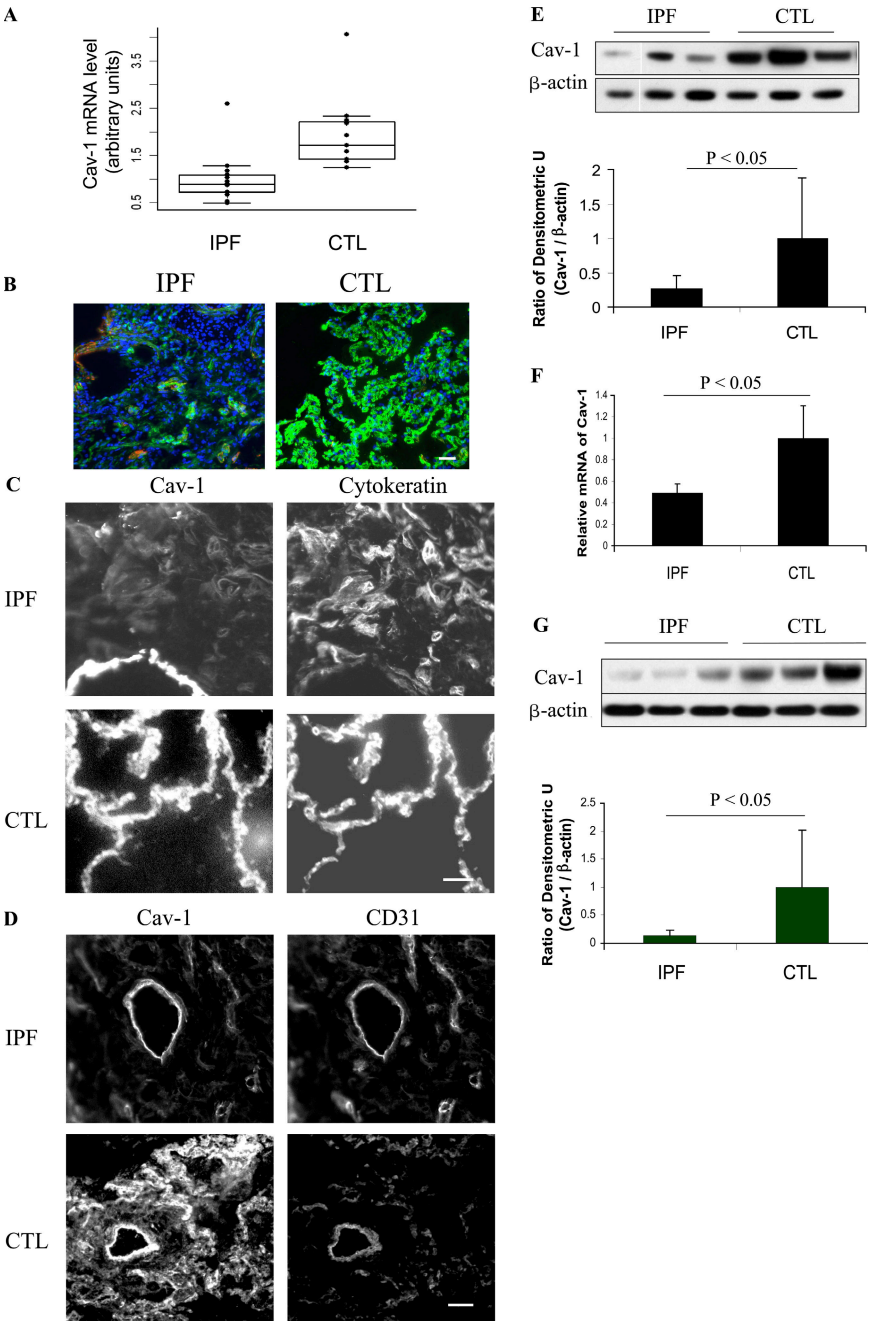

Figure 1. Altered cav-1 expressions in IPF patients. (A) Microarray analysis of cav-1 mRNA reveals a significant reduction (P = 0.000087, fold 0.5) in IPF patients (n = 13) compared with controls (n = 11). Boxes indicate the middle two quartile values, with the median values shown. Error bars represent 1.5× the interquartile range. (B) Immunohistochemical analysis of cav-1 expression in lung tissue sections (cav-1, green; nucleus, blue; α-SMA, orange). One representative example out of seven for patient sample or control subjects is shown. Bar, 100 μm. Immunohistochemical analysis of cytokeratin 19 (C) and CD31 (D) and cav-1 expression in normal (CTL) and IPF lung tissue sections. One representative example out of three for patient sample or control subjects is shown. Bars: (C) 50 μm; (D) 100 μm. (E) cav-1 protein expressions as detected by immunoblot analysis in lung tissue samples from IPF patients (n = 7) and control subjects (n = 7). Three representative samples of patients and controls are shown. White lines indicate that intervening lanes have been spliced out. (F) cav-1 mRNA expressions were detected by Taqman PCR in pulmonary fibroblasts derived from IPF patients (n = 4) and control subjects (n = 5). (G) cav-1 and β-actin protein expressions were determined by immunoblot analysis in pulmonary fibroblasts derived from IPF patients (n = 4) and control subjects (n = 5). Three representative patients and control samples are shown. The differences in mRNA level of cav-1 expression were compared by the Student's t test. The differences in protein levels of cav-1 expression were compared by the Wilcoxon two-sample test. Differences were considered significant at $P < 0.05$. Data in E–G represent the mean ± SEM. CTL, control.

progression of the disease (9, 10). Although there is no known etiologic stimulus that initiates IPF, many investigators believe that endogenous and exogenous stimuli may injure the alveolar epithelium, followed by an abnormal repair process (11), including aberrant cytokines and growth factor production (10). TGF-β1 has been implicated as one of the mediators in the initiation and progression of fibrosis (12). TGF-β1 initiates the signal by binding to TGF-βRI and TGF-βRII. The binding activates serine/threonine kinases of TGF-βR complexes, which phosphorylate the immediate effectors, smad-2/3. After phosphorylation, the conformation of smad-2/3 changes thereby facilitates the binding with smad-4. The smad complex then translocates into the nucleus, where it acts to modulate the extracellular matrix (ECM) gene transcription. A variety of molecules are reported to regulate the TGF-β signaling, including the extracellular signal–regulated protein kinase (ERK)–MAPK pathway, IFN-γ, and the inhibitory protein, smad-7, which directly interacts with the receptor and inhibits the signaling (12).

Recently, cav-1 expression was demonstrated to be abnormal in experimental models of pulmonary fibrosis. Tourkina et al. found that cav-1 expression was low in bleomycin (BLM)-induced lung fibrosis tissue (13). Kasper et al. reported that cav-1 expression decreased with the treatment of $CdCl_2$ and TGF-β1 in rat lung slices in vitro (14). They also observed that type I pneumocytes lost their cav-1 expression in early stages in a rat model of irradiation-induced lung injury (15). BLM, the drug inducing pulmonary fibrosis in vivo, decreased cav-1 expression in cultured rat epithelial cells (16). Moreover, cav-1 has been implicated to associate with TGF-βRs in human endothelial cells (17). cav-1 also inhibits the phosphorylation of smad-2, disrupting its interaction with smad-4, and prevents nucleus translocation of the smad-2 complex via the scaffolding domain of cav-1 in the mouse fibroblast NIH3T3 (18). Together with the studies of cav-1 knockout mice, which develop lung fibrosis (19), we hypothesize that cav-1 plays a pivotal role in regulation of ECM production, and treatment increasing cav-1 expression might suppress the pathogenesis of pulmonary fibrosis.

In this study, we tested our hypothesis in several independent ways. We extensively investigated cav-1 expression in lung tissue and fibroblasts from IPF patients and control subjects. We report for the first time that cav-1 confers antifibrotic effects both in vitro and in vivo. Our data suggest that cav-1 is an important regulator in the pathogenesis of pulmonary fibrosis and a promising molecular target in the therapy for pulmonary fibrosis.

RESULTS

Altered expression of cav-1 in lungs of IPF patients

Given the reduced cav-1 expression in samples from experimental pulmonary fibrosis that has been previously reported (13–15), we determined whether expression of cav-1 was altered in patients with IPF. We analyzed cav-1 expression in a previously described gene-profiling dataset of IPF (20) and observed a twofold reduction in cav-1 mRNA in IPF lung tissues ($P = 0.000087$; Fig. 1 A). A similar decrease was found in another dataset (21) that we recently published. The reduction of cav-1 protein expression was confirmed by immunohistochemistry staining (Fig. 1 B) and quantified by densitometric analysis of immunoblots (Fig. 1 E). Among the 14 lung tissue samples examined (7 IPF patients and 7 control subjects), the mean cav-1 expression decreased by ∼73% in IPF patients compared with the controls ($P = 0.035$), as measured by the ratio of band densitometric units of cav-1 to β-actin.

To determine cell type–specific loss of cav-1 expression in the IPF lung, we performed double immunohistochemistry staining of cav-1 with CD31 or cytokeratin 19. As demonstrated in Fig. 1 C, the cells positive for cytokeratin 19, which is known as an epithelial cell marker, showed a markedly decreased cav-1 expression compared with normal tissue, whereas the cells positive for CD31, which is known as an endothelial cell marker, demonstrated no reduction of cav-1 levels compared with control tissue (Fig. 1 D).

We next examined cav-1 expression in pulmonary fibroblasts by Taqman RT-PCR and immunoblot analysis. A marked reduction of cav-1 mRNA level was observed in pulmonary fibroblasts derived from IPF patients ($n = 4$) compared with control subjects ($n = 5$; Fig. 1 F). Similarly, cav-1 protein expression was also decreased significantly in IPF ($n = 4$) compared with control ($n = 5$) fibroblasts ($P = 0.014$; Fig. 1 G).

cav-1 gene transfer via adenovirus suppresses BLM-induced pulmonary fibrosis

To better understand the function of cav-1 in the fibrotic process, we tested the regulatory effects of cav-1 on BLM-induced pulmonary fibrosis in vivo. We constructed an adenovirus vector, which effectively transferred the *cav-1* gene into the lung tissue by intratracheal instillation (Fig. S1, available at http://www.jem.org/cgi/content/full/jem.20061536/DC1). The mice were infected with ad–cav-1, ad-lacZ, or saline 2 d before BLM or saline administration. Lung tissue was harvested 2 wk after injury and subjected to a variety of analyses.

For groups without BLM treatment, alveolar architecture was preserved (Fig. 2, A and B; and Fig. S2, available at http://www.jem.org/cgi/content/full/jem.20061536/DC1). No significant differences were observed among the saline, ad-lacZ, and ad–cav-1 groups (mean fibrosis scores: 0.12 ± 0.12, 0.49 ± 0.43, and 0.56 ± 0.06, respectively; $P = 0.162$; Fig. 2 C). Similarly, collagen accumulation, an index of lung fibrosis as determined by the measurement of hydroxyproline content, was basally low in these controls (111.58 ± 18.9, 133.6 ± 24.2, and 144.2 ± 27.7 μg, respectively; $P = 0.1987$; Fig. 2 D). Consistently, immunoblots of the homogenized protein of lung tissue demonstrated low basal ECM production and undetectable smad-2 activation (Fig. 2 E). TGF-β1, one of the key cytokines involved in pulmonary fibrosis (12), was observed to have low basal levels by ELISA in all three groups (Fig. 2 F).

In contrast, for groups with BLM treatment, lung tissue sections in both saline- and ad-lacZ–instilled groups showed

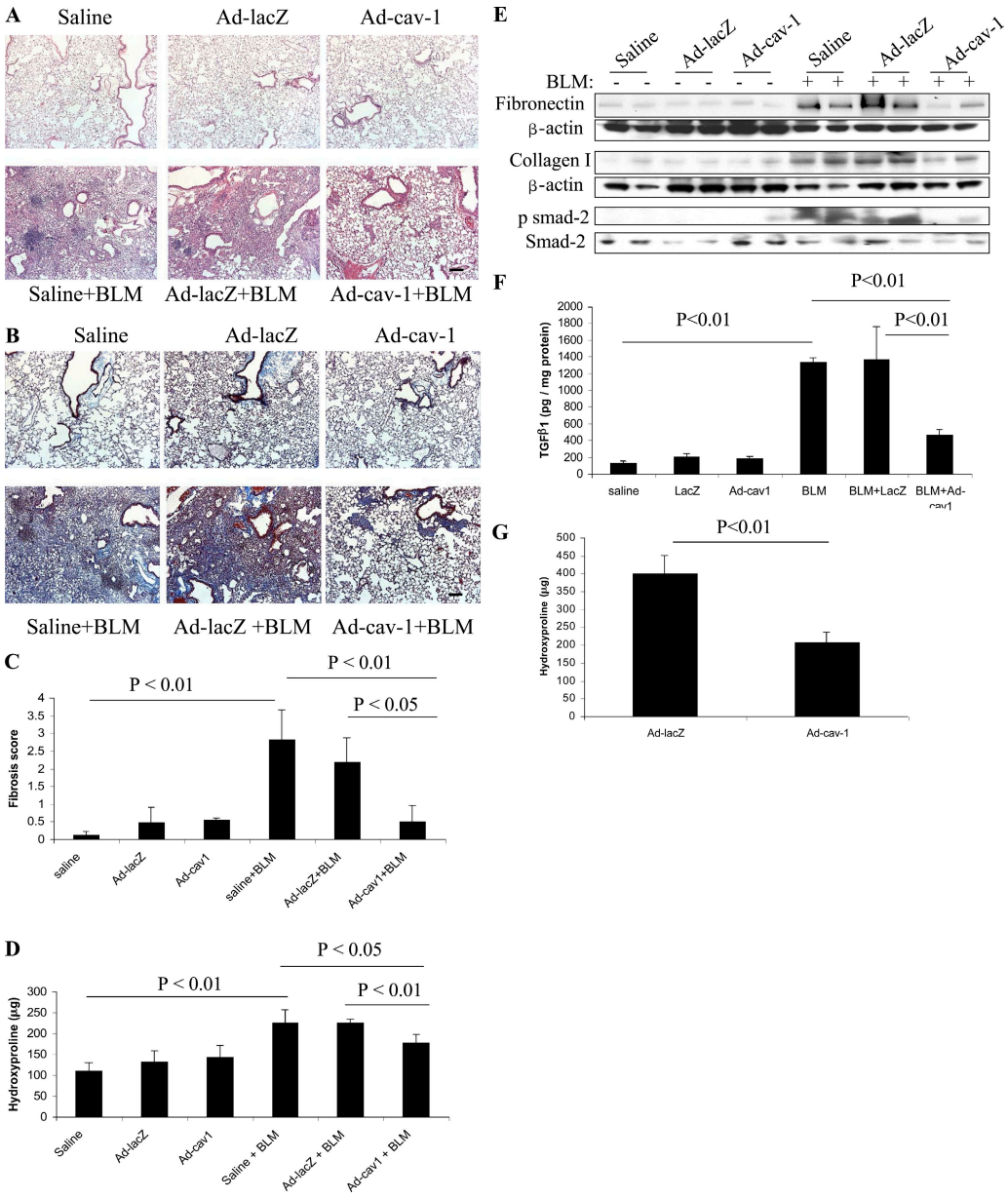

Figure 2. cav-1 suppresses BLM-induced pulmonary fibrosis. The C57BL/6 mice infected with ad–cav-1, ad-lacZ, or saline were treated with BLM for 14 d. The lungs were harvested and subjected to (A) H&E staining and (B) Masson trichrome staining of the right lung tissue. One representative example out of four or five is shown for each group in A and B. Bars, 200 μm. (C) Histology grade score analysis of the tissue sections (n = 4 and 5 for groups without and with BLM, respectively). (D) Hydroxyproline content determination of the left lung (n = 4 and 5 for groups without and with BLM, respectively). Data in C and D represent the mean ± SEM. (E) ECM deposition and smad-2 activation in the whole lung as determined by immunoblot analysis. (F) TGF-β1 content determination by ELISA of the homogenized protein of the whole lung (n = 3 for each group). (G) Hydroxyproline content determination of the whole lung 7 d after ad–cav-1 infection and 14 d after BLM instillation (n = 3 for each group). Data in F and G represent the mean ± SEM.

extensive patchy areas of regional interstitial fibrosis with marked disruption of the alveolar unit, increased thickening of the interstitium, and inflammation. However, in the ad–cav-1 group, the structural integrity of the lung was less severely affected, with less evidence of fibrotic obliteration, destruction of alveolar units, and inflammation cell infiltration (Fig. 2, A and B; and Fig. S2). The mean fibrosis score was significantly reduced in the ad–cav-1 group compared with the lacZ and saline groups (2.83 ± 0.85, 2.18 ± 0.7, and 0.52 ± 0.45 in the saline, ad-lacZ, and ad–cav-1 groups, respectively; $P = 0.0056$ overall; $P = 0.0009$ for lacZ and cav-1; Fig. 2 C). The hydroxyproline content was increased after BLM treatment in both the saline and ad-lacZ groups, whereas the ad–cav-1 group had a markedly reduced

hydroxyproline level (226.1 ± 29.7, 226.8 ± 8.2, and 178.4 ± 19.7 μg in the saline, ad-lacZ, and ad–cav-1 groups, respectively; P = 0.0048 overall; P = 0.001 for lacZ and cav-1; Fig. 2 D). Furthermore, immunoblot analysis revealed that ad–cav-1 treatment dramatically suppressed fibronectin and collagen deposition compared with the lacZ group (Fig. 2 E). As expected, TGF-β1 also increased with the development of fibrosis after BLM administration in both the saline and ad-lacZ groups, whereas it was significantly decreased in the ad–cav-1 infection group (Fig. 2 F). The smad-2 phosphorylation induced by BLM was also markedly diminished by ad–cav-1 infection (Fig. 2 E).

To explore the therapeutic potentials of ad–cav-1, we infected the mice with ad–cav-1 or ad-lacZ 7 d after BLM instillation. 1 wk later, the whole lung was subjected to hydroxyproline content determination. As shown in Fig. 2 G, ad–cav-1 infection suppressed hybroxyproline deposition compared with ad-lacZ infected mice (400.4 ± 51.1 and 208.9 ± 28.4 μg in the ad-lacZ and ad–cav-1 groups, respectively; P = 0.0048; Fig. 2 G).

TGF-β1 regulates cav-1 expression in pulmonary fibroblasts

TGF-β1 is one of the key cytokines involved in pulmonary fibrosis (12). Its level, contrary to cav-1 expression, increases considerably in active fibrotic areas (12), which leads to the hypothesis that TGF-β1 might be one of the negative regulators of cav-1 expression. To test this hypothesis, we administered TGF-β1 to human primary pulmonary fibroblasts and MRC-5, a human pulmonary fibroblast cell type, and analyzed the expression of cav-1. As detected by Taqman RT-PCR, mRNA of cav-1 markedly decreased in primary fibroblasts (P = 0.0024) and in MRC-5 (P = 0.0002; Fig. 3 A) after 1 d of treatment with TGF-β1. We also observed decreased cav-1 protein levels after TGF-β1 treatment in a time- and dose-dependent manner (Fig. 3, B and C).

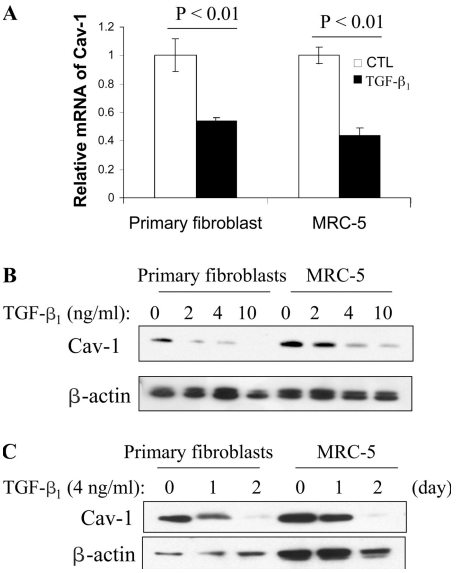

Figure 3. TGF-β1 regulates cav-1 expression. (A) Human primary pulmonary fibroblasts and MRC-5 cells were treated with 4 ng/ml TGF-β1 for 24 h. cav-1 mRNA levels were determined by Taqman PCR. Data represent the mean ± SEM. (B) The same cells were treated with different concentrations of TGF-β1 for 24 h (C) or treated with 4 ng/ml TGF-β1 for 1 and 2 d. cav-1 protein levels were determined by immunoblot analysis. Data are representative of three independent experiments.

cav-1 suppresses TGF-β1–induced ECM production in pulmonary fibroblasts

To delineate the mechanism of the antifibrotic effects of cav-1 observed in the in vivo studies (Fig. 2), we used an in vitro model to test the effects of cav-1 on TGF-β_1–induced ECM production with both gain of function and loss of function experiments. Three independent experiments were shown for each condition (one representative is shown in Fig. 4; see Fig. S4 for the other two). Densitometric quantification and statistical analysis were performed. For gain of function experiments, we used the ad–cav-1 to up-regulate cav-1 expression in MRC-5. cav-1 expression markedly increased in a dose-dependent manner after ad–cav-1 infection (Fig. S3 A, available at http://www.jem.org/cgi/content/full/jem.20061536/DC1), which lasted until the fourth day with optimal cav-1 expression at 2 d after infection (Fig. S3 B). Using this adenovirus, we found that overexpressing cav-1 significantly suppressed the TGF-β1–induced ECM production, including collagen type I and fibronectin (Fig. 4 A and Fig. S4 A). It also inhibited fibroblast activation, indicated by α–smooth muscle actin (α-SMA) production (Fig. 4 A and Fig. S4 A) (22). This observation was further confirmed in MRC-5 cells that were stably transfected with the *cav-1* gene. Likewise, the production of collagen type I, fibronectin, and α-SMA stimulated by TGF-β1 were markedly reduced by cav-1 stable transfection compared with the vector-transfected control cells (Fig. 4 B and Fig. S4 B). We also performed loss of function experiments by transfection of siRNA targeting human cav-1, which effectively reduced cav-1 expression (Fig. S3 C). Importantly, down-regulation of cav-1 markedly enhanced the TGF-β1–induced productions of α-SMA, collagen type I, and fibronectin (Fig. 4 C and Fig. S4 C). Under nonstimulated conditions, the effects of cav-1 on fibronectin, collagen type I, and α-SMA production were not statistically significant (Fig. 4) with the exception of collagen type I production in MRC-5 stably transfected with the *cav-1* gene (P < 0.05; Fig. 4 B).

cav-1 modulates TGF-β1–induced smad signaling

To investigate the molecular mechanism of antifibrotic effects of cav-1, we determined the regulation of smad activation by cav-1 in MRC-5 with both gain and loss of function experiments. Overexpression of cav-1 in ad–cav-1–infected MRC-5 suppressed smad-2 phosphorylation and nucleus translocation. It also effectively attenuated smad-3 nucleus translocation while having negligible effects on smad-4/7 expression and smad-4 nucleus translocation (Fig. 5 A). Down-regulation of cav-1 by siRNA transfection increased smad-2 phosphorylation and smad-2/3 nucleus translocation (Fig. 5 B).

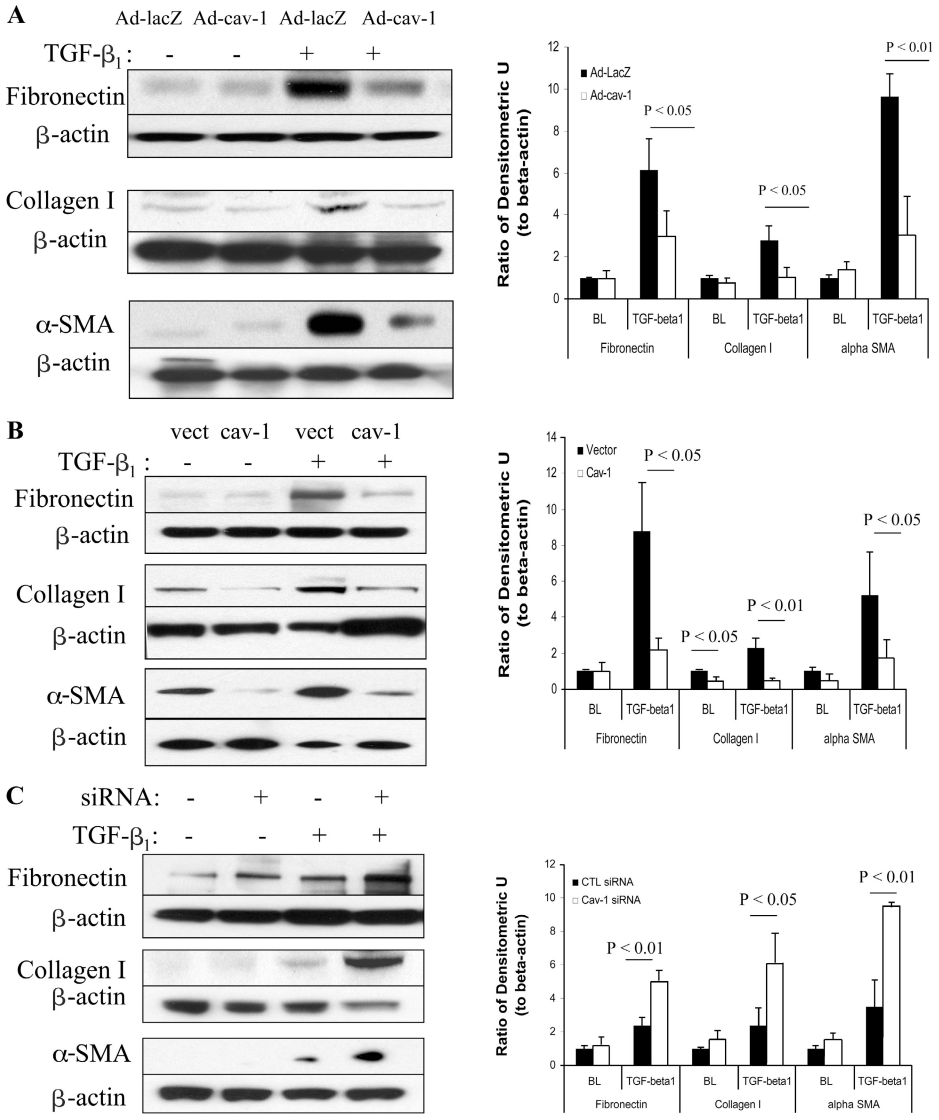

Figure 4. cav-1 modulates TGF-β1–induced ECM productions. (A) After adenovirus infection, 4 ng/ml TGF-β1 was added into MRC-5 for 2 d. ECM productions were determined by immunoblot analysis. (B) ECM productions in cav-1 stably transfected and control MRC-5 cells after 2 d of 4-ng/ml TGF-β1 treatment. (C) After siRNA transfection for 24 h, the MRC-5 cells were serum-starved overnight and treated with 4 ng/ml TGF-β1 for 2 d. ECM productions were determined by immunoblot analysis. Three independent experiments were performed, and one representative sample is shown. The differences in densitometric quantification of cav-1 expression were compared by the Student's *t* test. Differences were considered significant at $P < 0.05$. Data represent the mean ± SEM.

cav-1 modulates TGF-β1–induced ECM production via the c-Jun N-terminal kinase (JNK) pathway

MAPK pathways are reported to regulate TGF-β1 signaling and TGF-β1–induced ECM production by many investigators (23, 24). cav-1 has been shown to modulate MAPK activation in mesangial cells (25) and macrophages (26). In this paper, we hypothesized that cav-1 might regulate TGF-β1–induced ECM production via MAPK pathways in human lung fibroblasts. As demonstrated in Fig. 6 A, overexpressing cav-1 via ad–cav-1 substantially inhibited TGF-β1–induced ERK and JNK activation. There was no apparent induction of p38 phosphorylation by TGF-β1 in MRC-5. The involvement of ERK and JNK pathways was further explored using chemical inhibitors. Overexpressing cav-1 inhibited TGF-β1–induced ECM production in DMSO samples. In contrast, PD 98059 (an inhibitor of MEK1 and an upstream kinase of ERK) and UO 126 (an inhibitor of MEK1/2 and an upstream kinase of ERK) administration abolished the modulation of cav-1 on collagen type I production while having a negligible effect on fibronectin production (Fig. 6 B). On the other hand, SP 600125 (a JNK1/2 inhibitor), eliminated the modulation of cav-1 on fibronectin production while having less effect on collagen type I modulation (Fig. 6 B). Furthermore, pulmonary fibroblasts isolated from

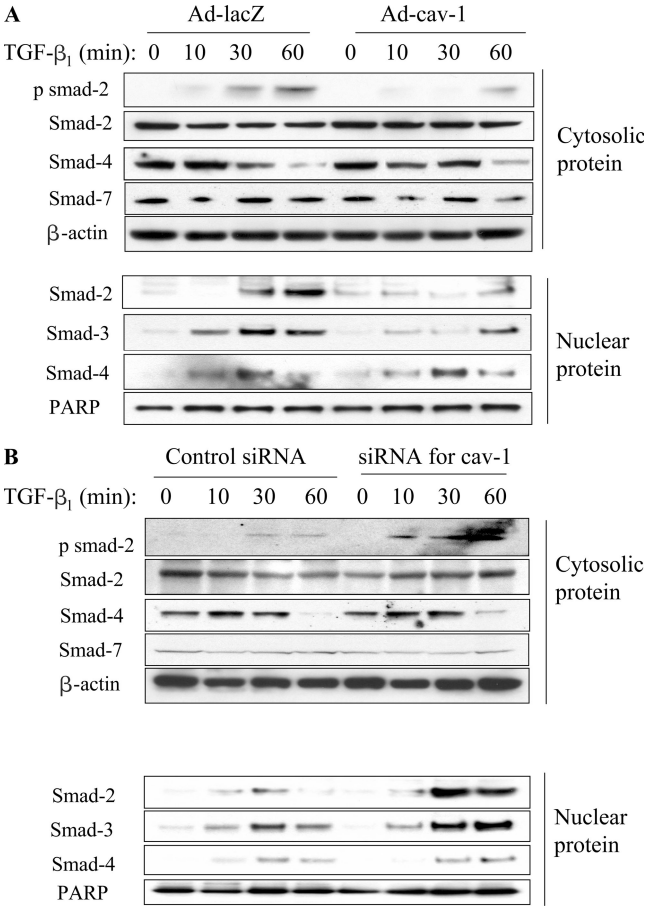

Figure 5. cav-1 modulates smad activation. Immunoblot analysis of smad-2 phosphorylation; smad-4 and smad-7 expressions in cytosolic extracts; and smad-2/3 and smad-4 existences in nuclear extracts under different conditions in MRC-5. (A) Cells were infected with ad–cav-1 and ad-lacZ and (B) transfected with siRNA targeting cav-1 and control for 24 h. The cells were serum-starved overnight and treated with TGF-β1 for 0, 10, 30, and 60 min. Data are representative of three independent experiments.

JNK1-null mice did not exhibit differences in TGF-β1–stimulated fibronectin production between ad-lacZ and ad–cav-1 infection compared with the fibroblasts isolated from JNK1 wild-type littermates (Fig. 6 C). These data suggest that cav-1 modulates TGF-β1–induced collagen type I production via the ERK1 pathway while modulating TGF-β1–induced fibronectin production via the JNK1 pathway.

JNK1-null mouse fibroblasts showed similar suppressions of smad-2 phosphorylation and smad-2/3 nucleus translocation, mimicking the effects of overexpressing cav-1 (Fig. 6 D), suggesting that cav-1 regulates smad-2/3 activation via the JNK1 pathway. To clarify this hypothesis, cav-1 was overexpressed in JNK1 wild-type and null fibroblasts by adenovirus infection. As expected, cav-1 markedly suppressed smad-2 phosphorylation and smad-2/3 nucleus translocation in wild-type fibroblasts (Fig. 6 E). Meanwhile, in JNK1-null fibroblasts, overexpressing cav-1 did not reduce smad-2 phosphorylation and nucleus translocation, whereas it still suppressed smad-3 nucleus translocation (Fig. 6 E).

To further investigate the role of JNK in vivo, we performed immunochemical analysis with the BLM-treated lung fibrosis tissue. As shown in Fig. 6 F, the phosphorylated JNK level was dramatically high in saline and lacZ mice, whereas ad–cav-1 infection markedly attenuated phospho-JNK. Moreover, JNK was highly activated in IPF tissues compared with the controls (Fig. 6 G), indicating its pivotal role in IPF development.

DISCUSSION

Because IPF shows a distinct histopathology of usual interstitial pneumonia, a commonly held view is that persistent interstitial inflammation leads to and modulates the development of fibrosis (27). This hypothesis is applied in clinical settings in that antiinflammatory therapies combined with immunosuppressive therapy are major strategies used in treating IPF. However, the outcome is still poor (11). A recent hypothesis has been advanced by Selman et al. and others that IPF is an epithelial-fibroblastic disease (28). Alveolar epithelial cell injury and activation will release many fibrogenic mediators, which lead to the transformation of fibroblasts to myofibroblasts and the formation of fibroblast-myofibroblast foci that is characterized by fibroblast-myofibroblast migration and proliferation, decreased apoptosis, and enhanced release of fibrogenic growth factors (e.g., TGF-β1) (28).

We observed that cav-1 was highly expressed in epithelial and endothelial cells in the normal lung, whereas in the IPF lung the cav-1 levels were reduced dramatically in epithelial cells, as evident by the immunohistochemical analysis. We noticed that reduced levels of cav-1 occurred in areas with minimal α-SMA staining. Together with a previous report that reduced cav-1 expression occurred at early stages of irradiation-induced pulmonary fibrosis in a rat model, when no apparent histopathology changes were observed (15), we hypothesized that the decreased cav-1 level might be an early event and indicator of the impaired cellular functions of epithelial cells in the initiation of IPF pathogenesis. However, we do not rule out the possibility that this phenomena also happens in later stages of fibrosis. The expression of cav-1 was also considerably reduced in fibroblasts derived from IPF patients. Interestingly, lung fibroblasts isolated from scleroderma patients with pulmonary fibrosis also showed a decreased expression of cav-1 (13), suggesting that the reduced cav-1 level occurs in other pulmonary fibrotic disorders, such as scleroderma. Consistent with the reduced cav-1 level in IPF, myofibroblasts were reported to be lacking caveolae, as revealed by electron microscopy (29). Consequently, decreased cav-1 levels might lead to hyperactive TGF-β1 signaling in fibroblasts and increased TGF-β1 secretion. The expression of mRNA was in accordance with the protein level, suggesting that cav-1 is primarily regulated at the transcriptional level. We noticed the standard deviation of cav-1 expression in control samples was high, which can be explained by the wide range of individual variance. However, cav-1 expression in

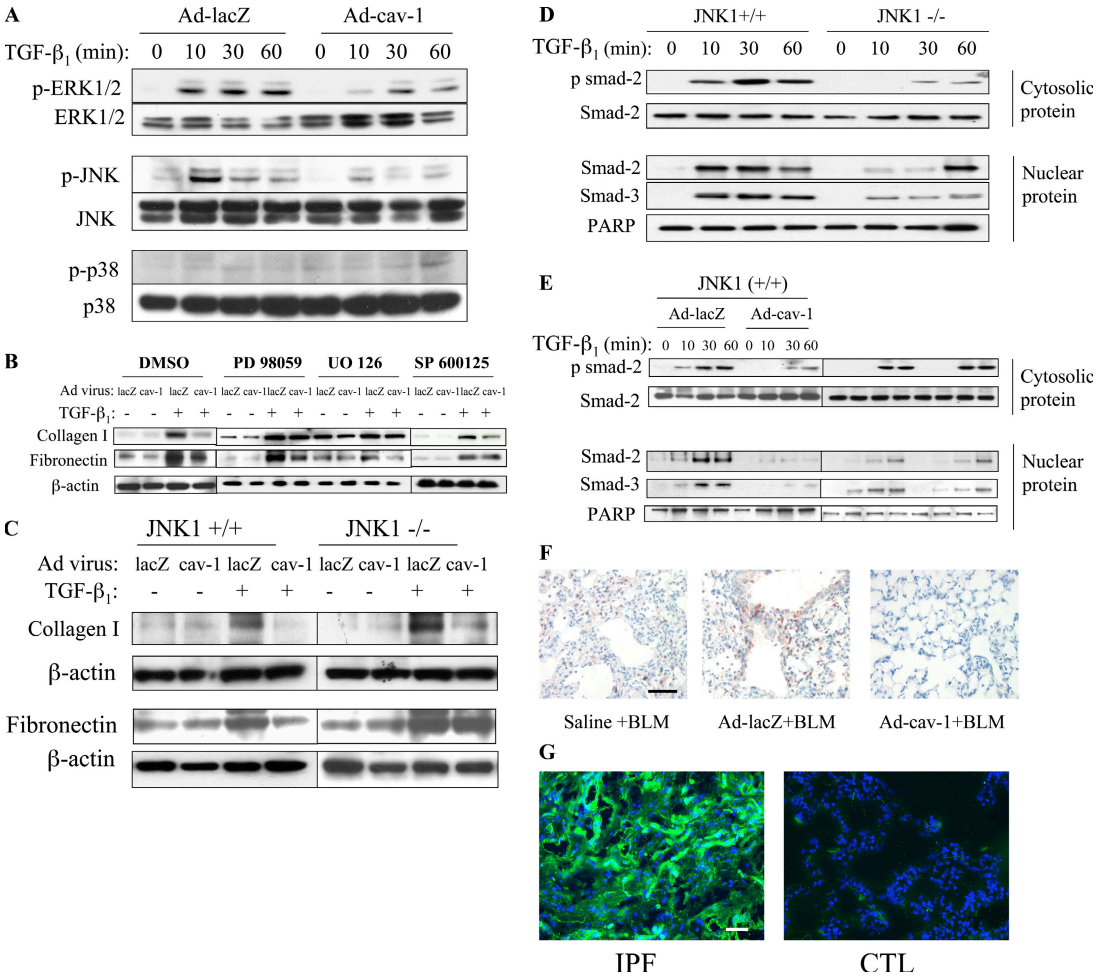

Figure 6. MAPK pathways are involved in ECM regulation of cav-1. (A) Immunoblot analysis of TGF-β1–stimulated MAPK activation for 0, 10, 30, and 60 min in MRC-5 cells infected with ad–cav-1 or ad-lacZ. (B) Immunoblot analysis of TGF-β1–stimulated ECM production in MRC-5 cells infected with ad–cav-1 or ad-lacZ. The cells were pretreated with DMSO or PD 98059, or UO 126 or SP 600125 for 1 h, and administrated with TGF-β1 for 2 d. (C) Immunoblot analysis of TGF-β1–stimulated ECM production in pulmonary fibroblasts isolated from JNK1 (+/+) and (−/−) mice infected with ad–cav-1 or ad-lacZ. (D) Immunoblot analysis of smad-2 phosphorylation in cytosolic extracts and smad-2/3 existences in nuclear extracts. (E) Immunoblot analysis of smad-2 phosphorylation in cytosolic extracts and smad-2/3 existences in nuclear extracts in JNK1 wild-type and null fibroblasts infected with ad–cav-1 or ad-lacZ. Data are representative of three independent experiments in A–E. (F) Immunohistochemical analysis of JNK phosphorylation in paraffin-embedded lung tissue slices treated with BLM and infected with ad-lacZ or ad–cav-1 or instilled with saline. Brown indicates phospho-JNK–positive cells. One representative example out of five is shown. Bar, 100 μm. (G) Immunohistochemical analysis of JNK phosphorylation in frozen lung tissue slices from IPF patients and control subjects (phospho-JNK, green; nucleus, blue). One representative example out of seven for patients or controls is shown. Bar, 100 μm.

IPF samples was consistently low with a narrow range of variance. We found that TGF-β1 markedly decreased cav-1 expression in a dose- and time-dependent manner in human pulmonary fibroblasts, whereas TGF-β1 was demonstrated to be produced at the sites of active fibrosis, and its level in the lung was reported to be proportionate to the degree of fibrosis generated (12). Therefore, the increased levels of TGF-β1 might contribute to the cell type–specific attenuation of cav-1 expression in lung tissues of IPF patients.

IPF is a disease with substantially high morbidity and mortality. To date, no effective approaches are available to reverse the development of pulmonary fibrosis. In this study, we found that cav-1, the caveolae marker protein involved in many signal pathways, shows promise for slowing the progression of pulmonary fibrosis. In the BLM-induced pulmonary fibrosis model in vivo, overexpression of cav-1 by adenoviral gene transfer strikingly diminished the lung fibrosis scores and hydroxyproline content compared with lacZ virus, accomplished by attenuated collagen deposition, reduced fibronectin production, less TGF-β1 secretion, and smad-2 phosphorylation. Moreover, we infected the mice with ad–cav-1 7 d after BLM injury, when the fibrosis was already initiated and minor lung injury can be detected (30). cav-1 was still able to suppress the fibrosis development, as

demonstrated by the reduction of the hydroxyproline deposition. As we noticed, the reduction of hydroxyproline content in the left lung was not as impressive as histology examination scores of the right lung. This might be caused by the low sensitivity of the assay or uneven distribution of the virus and BLM in the left and right lung, which is associated with intratracheal administration through the mouth into asymmetric lungs of mice.

TGF-β1 is a major pivotal fibrogenic factor involved in IPF (22). It promotes myofibroblast transformation, which is responsible for secreting large amount of ECM, and presents only in fibrotic lung tissue but not in normal lung tissue (22). It suppresses ECM degradation through the regulation of matrix metalloproteases and their inhibitors (31). TGF-β1 causes minor inflammation but marked progressive fibrosis in the lung. It has many diverse functions, including chemoattractant and mitogenic activities and the regulation of lung inflammation and functions of epithelial cells, which further affect the fibrotic process through autocrine or paracrine mechanisms (12). Transfer of the TGF-β1 gene into rat lungs via an adenoviral vector can induce a severe and progressive lung fibrosis (32). Blocking TGF-β1 can effectively reduce the fibrosis in different animal models (12). Inhibition of TGF-β1 signaling was capable of slowing the progression of IPF when administered to patients (33). In this paper, using several independent and complementary approaches, we demonstrated that cav-1 modulated TGF-β1 signaling and that it induced ECM productions, including collagen type I and fibronectin in human pulmonary fibroblasts. We chose the TGF-β1 stimulation fibrosis model instead of the unstimulated state because that was more similar to the pathological and physiological conditions in pulmonary fibrosis development. It was recently reported that inhibition of cav-1 expression by siRNA increased baseline collagen accumulation in normal lung fibroblasts (13). Our results show that the changing cav-1 expression does not significantly affect baseline fibronectin, collagen, and α−SMA production in MRC-5. The only significant baseline change was that cav-1 stably transfected MRC-5 had less collagen type I accumulation. Note that although the baseline level of collagen type I was reduced by cav-1 stable transfection, cav-1 more dramatically attenuated ECM accumulations in the TGF-β1–stimulated state.

Given the previous report that cav-1 interacted with TGF-βRI and transfection of a HA-tag cav-1–inhibited smad-2 phosphorylation in NIH3T3 cells (18), we postulated that cav-1 might modulate smad activity. The effect of cav-1 on smad-3, -4, and -7 has not, to our knowledge, previously been examined. Using adenovirus and siRNA transfection, cav-1 was demonstrated to suppress TGF-β1–induced smad-2 phosphorylation, similar to the earlier studies (18). cav-1 was also found to suppress smad-3 nucleus translocation but had no apparent effects on smad-4/7 expression.

The family of MAPKs consists of three known subfamilies, including ERK1/2, JNK1/2, and p38. These MAPKs have been reported to regulate TGF-β1–induced ECM production and pulmonary fibrosis (20, 21), greatly depending on the cell types and experimental conditions. We examined the role of the MAPK signaling cascades in mediating the effect of cav-1 on collagen and fibronectin synthesis. In the present studies, ERK and JNK were induced rapidly by TGF-β1, whereas p38 seemed to have no apparent induction. Up-regulation of cav-1 by adenoviral infection markedly attenuated the ERK and JNK phosphorylation, especially JNK phosphorylation 10 min after treatment. cav-1 has been demonstrated to regulate ERK1/2 activation in a variety of cells (1, 5, 6). It has also been shown that ERK localizes in caveolae and directly interacts with cav-1 (6). With respect to ECM regulation, we find that inhibiting ERK1 or ERK1/2 selectively blocks the reduction effects of cav-1 on collagen type I but not fibronectin production. These data were consistent with previous findings that ERK1/2 regulated collagen expression in pulmonary and dermal fibroblasts (34, 35), and that ERK1/2 mediated cav-1 modulation of collagen type I production in nonstimulated states (13).

Interestingly, inhibition of the JNK pathway by the chemical inhibitor SP 600125 or genetic knockout selectively blocks the reduction effects of cav-1 on fibronectin production but not collagen type I. In a human fibrosarcoma cell line, a similar finding was reported that JNK activation was essential for TGF-β1–stimulated fibronectin production, as stable transfection of the dominant-negative mutant of JNK1 had markedly suppressed TGF-β1–stimulated fibronectin mRNA and protein expression (36). Further investigation using JNK1-null fibroblasts demonstrated the same reduced smad-2 phosphorylation and decreased smad-2/3 nucleus translocations compared with the wild-type fibroblasts. In JNK1-null cells, cav-1 lost the ability to suppress smad-2 activation, while it was still capable of inhibiting smad-3 activation. Moreover, phospho-JNK staining was markedly reduced in ad–cav-1–infected BLM- injured mice lung samples compared with lacZ or saline samples. Together with the fact that JNK was highly activated in IPF lung tissues, our data indicate that cav-1 regulates TGF-β1–induced fibronectin production via the JNK pathway, possibly via the modulation of smad-2 phosphorylation and nucleus translocation (Fig. 7).

In summary, we have demonstrated that cav-1 is capable of inhibiting the production of matrix molecules by fibroblasts, and exogenous transfer of cav-1 can inhibit the pulmonary fibrotic response in a BLM rodent model. We have also shown that cav-1 inhibited TGF-β1–induced collagen type I production via the ERK pathway and fibronectin production via JNK pathway. We found that cav-1 mRNA and protein expression were low in the lung tissues and fibroblasts of IPF patients. We postulate that one of the mechanisms for the phenomenon is through TGF-β1, which was shown to be an effective regulator of cav-1 expression in pulmonary fibroblasts. We delineated that the inhibition of smad-2 activation was by the cav-1–regulated JNK pathway. Our study strongly supports a pivotal role for cav-1 in ECM regulation and suggests a novel therapeutic target for patients with pulmonary fibrosis.

MATERIALS AND METHODS

Tissues, cell cultures, animals, and reagents. This study was approved by the Institutional Review Board for Human Subject Research at the University of Pittsburgh. Human lung tissues were obtained from the tissue bank and core facility at the University of Pittsburgh. Diagnosis of IPF was supported by history, physical examination, pulmonary function studies, chest high-resolution computed tomography, and bronchoalveolar lavage findings and corroborated by open lung biopsy. The morphologic diagnosis of IPF was based on typical microscopic findings consistent with usual interstitial pneumonia. The patients fulfilled the criteria of the American Thoracic Society and European Respiratory Society (37). Age-, race-, and sex-matched control samples, including normal histology lung samples from patients with lung cancer, were obtained from the Pittsburgh Tissue Bank. Primary pulmonary fibroblasts were derived from a subset of the lung tissues from IPF patients and controls that were used for immunoblot and microarray studies. The cells were maintained in 10% FBS DMEM with 50 μg/ml gentamicin. Primary pulmonary fibroblasts were isolated from JNK1$^{-/-}$ mice and wild-type littermates, as previously described (38). Human fetal pulmonary fibroblasts (MRC-5; American Type Culture Collection) were maintained in 10% FBS DMEM. MRC-5 cells were cotransfected (1:10) with pcDNA3.0 containing the neomycin selection marker, the expression vector pCAGGS containing cav-1 cDNA in the sense orientation, or with the pCAGGS control vector. Transfected cells were grown in 10% FBS DMEM containing 200 μg/ml G418. Cultures were maintained at 37°C in a humidified atmosphere of 5% CO_2 and 95% air. Cell culture reagents were purchased from Invitrogen. The cells were serum starved before TGF-β1 (R&D Systems) stimulation. TGF-β1 was reconstituted in 4 mM of sterile HCl containing 0.1% BSA. C57BL/6 mice were purchased from the Jackson Laboratory and acclimated for 1 wk before experiments. All animals were housed in accordance with guidelines from the American Association for Laboratory Animal Care and Research Protocols and were approved by the Animal Care and Use Committee of the University of Pittsburgh School of Medicine. 10 μM each of PD 98059, UO 126, and SP 600125 (Calbiochem) were dissolved in DMSO. Those reagents were added to the culture medium 1 h before other treatments.

cav-1 adenovirus construction and infection. cav-1 cDNA (provided by F. Galbiati, University of Pittsburgh, Pittsburgh, PA) was inserted into a pAdlox plasmid. cav-1 and lacZ adenovirus productions were performed by the Vector Core Facility at the University of Pittsburgh. For cell infection, 2×10^5 MRC cells were cultured in sixwell plates and exposed to 2×10^7 PFU of each virus in 1 ml of serum-free medium for 4 h. The cells were washed and incubated in serum-containing media for 36 h. The cells were subjected to other treatments as indicated in the figure legends. For animal infection, 10^{11} virus particles of each virus in 50 μl of saline were administrated intratracheally per mouse.

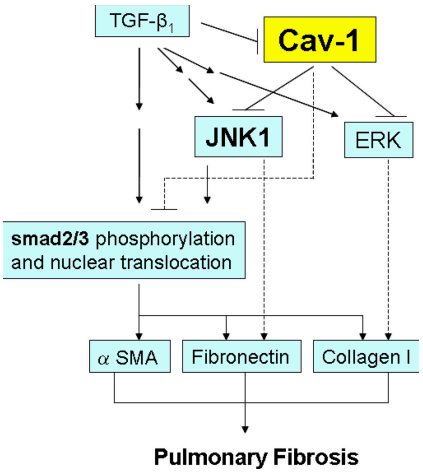

Figure 7. Summary of the role of cav-1 in pulmonary fibrosis. cav-1 modulates TGF-β1–induced JNK1 and smad-2/3 activity and inhibits α-SMA, fibronectin, and collagen type I production.

BLM administration. After 2 d of adenovirus infection, the mice were lightly sedated with isofluorane. A dose of 3 U/kg BLM (Bristol-Myers Squibb) in 50 μl of sterile saline was administered intratracheally by canulation of the trachea via the mouth with a 20-gauge feeding needle.

Histopathology. The right lungs were fixed in 10% formaldehyde for 24 h and processed for paraffin embedding. Sections of lung were stained with routine hematoxylin and eosin (H&E) or with a Masson trichrome stain to assess the degree of fibrosis. The extent of lung fibrosis was graded by a pathologist (T.D. Oury) in a blinded manner on a scale of 0 (normal lung) to 4 as previously described (39, 40). The major criteria examined included interstitial thickening of alveolar or bronchiolar walls, collagen deposition, and inflammatory cell infiltration.

Hyproxyproline assay. After 14 d of BLM administration, the left lungs were harvested and dried at 110°C until a constant weight was obtained. For the therapeutic experiment, mice were infected with ad–cav-1 1 wk after BLM injury. The whole lung was harvested 1 wk later. The dried lung was hydrolyzed under vacuum in a glass vial containing 1 ml of 6 N HCl at 110°C overnight. The samples were lyophilized and assayed for hydroxyproline content using a chloramine-T method, as previously described (39, 40).

TGF-β1 determination. After different treatments with adenovirus and BLM as indicated in the preceding sections, the entire lung was harvested and homogenized as previously described (41). The levels of cytokine TGF-β1 were measured by ELISA kits (R&D Systems) according to the manufacturer's instructions.

Synthesis and transfection of siRNA. siRNA sequences targeting human cav-1 gene (AACCAGAAGGGACACACAGTT) were synthesized (Dharmacon, Inc.) (42). The sequence (AACGCGCACACCAAGGAGATT) targeting the mice cav-1 gene with no apparent effects in human cells was used as a negative control. For transfection, cells were plated on sixwell plates. Transfections were performed with TransIT-TKO reagent (Mirus Corp.), as directed by the manufacturer. Each well received 10 nM siRNA in a volume of 1 mL in triplicate. Other treatment was added after 24 h of transfection.

Immunohistochemistry. In brief, lung tissues were fixed in 2% paraformaldehyde for 2 h and in 30% sucrose overnight. The tissues were frozen in liquid nitrogen and subjected to immunohistochemistry. The 6-μm tissue sections were washed three times in 0.5% BSA (Sigma-Aldrich) and blocked for 1 h in 2% BSA. After three washings of the samples in 0.5% BSA, tissue sections were incubated with the antibody specific for cav-1 (Santa Cruz Biotechnology, Inc.), phospho-JNK (Cell Signaling Technology, Inc.), α-SMA (ARP American Research Products, Inc.), CD31 (Abcam), or cytokeratin 19 (Chemicon) for 1 h. The samples were washed five times in BSA and incubated with Cyr3 or an FITC 488–conjugated goat anti–rabbit Fab fragment (Jackson ImmunoResearch Laboratories) for 1 h. For mice samples, after five washings in BSA, the sections were incubated with the Alexa Fluor 647 phalloidin (Invitrogen) for 1 h. Samples were washed five times in BSA and PBS. Hoechst dye (Sigma-Aldrich) was added for 30 s, and samples were washed in PBS and mounted. Tissue sections were viewed with a fluorescent microscope (BX51; Olympus). For paraffin-embedding lung samples, immunohistochemistry staining of phospho-JNK was performed as the manufacturer recommended (Cell Signaling Technology, Inc.).

Immunoblotting analysis. We performed an immunoblot analysis, as described previously (26). Nuclear protein extracts were isolated as previously described (26). Immunoreactive bands were quantified using a molecular

image system (GS-525; Bio-Rad Laboratories). Specific protein expression levels were normalized to the β-actin protein signal on the same nitrocellulose membrane.

Oligonucleotide microarrays. The samples and methods for the generation of microarray data have been previously described (20). In brief, 13 samples obtained from surgical remnants of biopsies or lungs explanted from patients with IPF that underwent pulmonary transplant and 11 normal histology lung samples resected from patients with lung cancer were obtained from the tissue bank of the Department of Pathology at the University of Pittsburgh. Total RNA was extracted and used as a template to generate double-stranded cDNA and biotin-labeled cRNA, as recommended by the manufacturer of the arrays and previously described (20). Fragmented cRNA was hybridized to slides (CodeLink Uniset I; GE Healthcare). After hybridization, arrays were washed and stained with streptavidin–Alexa Fluor 647. The arrays were scanned using a microarray scanner (GenePix 4000B; Molecular Devices). Images were analyzed using an analysis suite (CodeLink Expression II; GE Healthcare). They were visually inspected for defects and quality control parameters as recommended by the manufacturer. Data files were imported into a microarray database, linked with updated gene annotations using SOURCE (http://genome-www5.stanford.edu/cgi-bin/SMD/source/sourceSearch), and median scaled. Based on our previous experience, all expression levels below 0.01 were brought to 0.01. The complete set of gene array data has been deposited in the National Center for Biotechnology Information Gene Expression Omnibus (http://www.ncbi.nlm.nih.gov/geo) under accession no. GSE2052, according to MIAME guidelines. The general approach to analysis was previously described (43).

Purification of RNA and quantitative RT-PCR. Total RNA was isolated from cells with TRIzol reagent using the manufacturer's protocol (Invitrogen) and further purified with an RNeasy Mini kit (QIAGEN). The RT was performed using Superscript II (Invitrogen) according to manufacturer's instructions. Isolated RNA was incubated with a random hexamer at 65°C for 5 min for annealing. The optimal RT reaction was then performed in 20-μl volumes consisting of 1× RT buffer, 1 μl of SuperScript II reverse transcriptase, 1 μl of RNaseOUT, 5 mM $MgCl_2$, 0.5 mM dNTP, 0.01 mM DTT, 5 μmol/L of random hexamers, and 500 ng of total RNA. Reactions were incubated at 25°C for 10 min, 48°C for 30 min, and 95°C for 5 min. "No RT" controls were performed in all samples using the same RT reaction mix but substituting DEPC-H_2O for SuperScript II reverse transcriptase. PCR primers, fluorogenic probes, and all other reagents were purchased from Applied Biosystems (human cav-1 and human β-glucuronidase) and used according to the manufacturer's protocol. Quantitative RT-PCR was performed in triplicate in 40-μl reaction volumes consisting of 1× PCR buffer A, 3.5 mM $MgCl_2$, 0.3 mM dNTP, 0.025 U/μl of AmpliTaq Gold, and 4 μl of the RT reaction. Two-step PCR cycling was performed as follows: 95°C for 12 min × 1 cycle, 95°C for 15 s, and 60°C for 1 min × 40 cycles. At the end of the PCR, baseline and threshold values were set in software (ABI 7700 Prism; Applied Biosystems), and the relative cav-1 expressions were calculated as previously described (44).

Statistical analysis. Statistical analysis of microarrays was performed using the ScoreGenes gene expression package (http://www.cs.huji.ac.il/labs/compbio/scoregenes), and data visualization was performed using GeneXPress (http://genexpress.stanford.edu) and Spotfire DecisionSite (version 8.0; Spotfire Inc.). p-values were calculated by multiple testing, as previously described (39). The differences in mRNA and protein levels of cav-1 expression in IPF and control samples were compared by the Wilcoxon two-sample test, because the data do not follow a normal distribution. The differences in mRNA levels of cav-1 expression in MRC-5 cells determined by Taqman RT-PCR were compared by the Student's *t* test, because the data follow a normal distribution. The normality of the dataset was tested by the Anderson-Darling goodness-of-fit test. For animal experiments, differences in measured variables between experimental and control groups were analyzed using analysis of variance (ANOVA). Groups containing multiple comparisons were assessed by ANOVA, and Bonferroni's correction was used in determining p-values. For statistical analysis of the densitometric quantification of in vitro ECM production, the Student's *t* test was used, because the data follow a normal distribution. All analyses were performed with SPSS for Windows (version 12.0.1) and were considered significant at $P < 0.05$.

Online supplemental material. Fig. S1 shows the cav-1 gene expression in mouse lung tissue after ad–cav-1 infection. Fig. S2 shows the low magnification picture of H&E and Masson trichrome staining of lung sections infected with ad–cav-1, ad-lacZ, or saline. Fig. S3 shows cav-1 expression in MRC-5 cells infected with ad–cav-1, stably transfected with cav-1 cDNA, or transfected with siRNA targeting cav-1. Fig. S4 shows the collagen type I, fibronectin, and α-SMA production in MRC-5 cells infected with ad–cav-1, stably transfected with cav-1 cDNA, or transfected with siRNA targeting cav-1. Online supplemental material is available at http://www.jem.org/cgi/content/full/jem.20061536/DC1.

We would like to express our deepest appreciation to all of the IPF patients at the Dorothy P. and Richard P. Simmons Center for Interstitial Lung Disease who kindly provided tissue samples for this study. We thank Dr. Ferruccio Galbiati for providing us with the cav-1 cDNA.

This work was supported in part by American Heart Association grants AHA0515312U and AHA0525552U (to X.M. Wang and H.P. Kim, respectively); a Young Investigator Award from the Pulmonary Fibrosis Foundation (to Y. Zhang); National Institutes of Health grants R01-HL060234, R01-HL55330, R01-HL079904, and P01-HL70807 (to A.M.K. Choi) and R01-HL073745-01 (to N. Kaminski); and by a generous donation from the Simmons family.

The authors declare that they have no competing financial interests.

Submitted: 21 July 2006
Accepted: 17 November 2006

REFERENCES

1. Anderson, R.G. 1993. Caveolae: where incoming and outgoing messengers meet. *Proc. Natl. Acad. Sci. USA*. 90:10909–10913.
2. Scherer, P.E., R.Y. Lewis, D. Volonte, J.A. Engelman, F. Galbiati, J. Couet, D.S. Kohtz, E. van Donselaar, P. Peters, and M.P. Lisanti. 1997. Cell-type and tissue-specific expression of caveolin-2. Caveolins 1 and 2 co-localize and form a stable hetero-oligomeric complex in vivo. *J. Biol. Chem.* 272:29337–29346.
3. Rothberg, K.G., J.E. Heuser, W.C. Donzell, Y.S. Ying, J.R. Glenney, and R.G. Anderson. 1992. Caveolin, a protein component of caveolae membrane coats. *Cell*. 68:673–682.
4. Tang, Z., P.E. Scherer, T. Okamoto, K. Song, C. Chu, D.S. Kohtz, I. Nishimoto, H.F. Lodish, and M.P. Lisanti. 1996. Molecular cloning of caveolin-3, a novel member of the caveolin gene family expressed predominantly in muscle. *J. Biol. Chem.* 271:2255–2261.
5. Okamoto, T., A. Schlegel, P.E. Scherer, and M.P. Lisanti. 1998. Caveolins, a family of scaffolding proteins for organizing "preassembled signaling complexes" at the plasma membrane. *J. Biol. Chem.* 273:5419–5422.
6. Mineo, C., G.L. James, E.J. Smart, and R.G. Anderson. 1996. Localization of epidermal growth factor-stimulated Ras/Raf-1 interaction to caveolae membrane. *J. Biol. Chem.* 271:11930–11935.
7. Liu, P., Y. Ying, Y.G. Ko, and R.G. Anderson. 1996. Localization of platelet-derived growth factor-stimulated phosphorylation cascade to caveolae. *J. Biol. Chem.* 271:10299–10303.
8. Khalil, N., and R. O' Connor. 2004. Idiopathic pulmonary fibrosis: current understanding of the pathogenesis and the status of treatment. *CMAJ*. 171:153–160.
9. Brown, K.K., and G. Raghu. 2004. Medical treatment for pulmonary fibrosis: current trends, concepts, and prospects. *Clin. Chest Med.* 25:759–772.
10. American Thoracic Society. 2000. Idiopathic pulmonary fibrosis: diagnosis and treatment. International consensus statement. *Am. J. Respir. Crit. Care Med.* 161:646–664.

11. Selman, M., V.J. Thannickal, A. Pardo, D.A. Zisman, F.J. Martinez, and J.P. Lynch III. 2004. Idiopathic pulmonary fibrosis: pathogenesis and therapeutic approaches. *Drugs*. 64:405–430.
12. Lasky, J.A., and A.R. Brody. 2000. Interstitial fibrosis and growth factors. *Environ. Health Perspect*. 108:751–762.
13. Tourkina, E., P. Gooz, J. Pannu, M. Bonner, D. Scholz, S. Hacker, R.M. Silver, M. Trojanowska, and S. Hoffman. 2005. Opposing effects of protein kinase Calpha and protein kinase Cepsilon on collagen expression by human lung fibroblasts are mediated via MEK/ERK and caveolin-1 signaling. *J. Biol. Chem*. 280:13879–13887.
14. Kasper, M., D. Seidel, L. Knels, N. Morishima, A. Neisser, S. Bramke, and R. Koslowski. 2004. Early signs of lung fibrosis after in vitro treatment of rat lung slices. *Histochem. Cell Biol*. 121:131–140.
15. Kasper, M., T. Reimann, U. Hempel, K.W. Wenzel, A. Bierhaus, D. Schuh, V. Dimmer, G. Haroske, and M. Muller. 1998. Loss of caveolin expression in type I pneumocytes as an indicator of subcellular alterations during lung fibrogenesis. *Histochem. Cell Biol*. 109:41–48.
16. Koslowski, R., K. Barth, A. Augstein, T. Tschernig, G. Bargsten, M. Aufderheide, and M. Kasper. 2004. A new rat type I-like alveolar epithelial cell line R3/1: bleomycin effects on caveolin expression. *Histochem. Cell Biol*. 121:509–519.
17. Schwartz, E.A., E. Reaven, J.N. Topper, and P.S. Tsao. 2005. Transforming growth factor-beta receptors localize to caveolae and regulate endothelial nitric oxide synthase in normal human endothelial cells. *Biochem. J*. 390:199–206.
18. Razani, B., X.L. Zhang, M. Bitzer, G. von Gersdorff, E.P. Bottinger, and M.P. Lisanti. 2001. Caveolin-1 regulates transforming growth factor (TGF)-beta/SMAD signaling through an interaction with the TGF-beta type I receptor. *J. Biol. Chem*. 276:6727–6738.
19. Drab, M., P. Verkade, M. Elger, M. Kasper, M. Lohn, B. Lauterbach, J. Menne, C. Lindschau, F. Mende, F.C. Luft, et al. 2001. Loss of caveolae, vascular dysfunction, and pulmonary defects in caveolin-1 gene-disrupted mice. *Science*. 293:2449–2452.
20. Pardo, A., K. Gibson, J. Cisneros, T.J. Richards, Y. Yang, C. Becerril, S. Yousem, I. Herrera, V. Ruiz, M. Selman, and N. Kaminski. 2005. Up-regulation and profibrotic role of osteopontin in human idiopathic pulmonary fibrosis. *PLoS Med*. 2:e251.
21. Selman, M., A. Pardo, L. Barrera, A. Estrada, S.R. Watson, K. Wilson, N. Aziz, N. Kaminski, and A. Zlotnik. 2006. Gene expression profiles distinguish idiopathic pulmonary fibrosis from hypersensitivity pneumonitis. *Am. J. Respir. Crit. Care Med*. 173:188–198.
22. Allen, J.T., and M.A. Spiteri. 2002. Growth factors in idiopathic pulmonary fibrosis: relative roles. *Respir. Res*. 3:13.
23. Choi, M.E. 2000. Mechanism of transforming growth factor-beta1 signaling. *Kidney Int. Suppl*. 77:S53–S58.
24. Yue, J., and K.M. Mulder. 2000. Activation of the mitogen-activated protein kinase pathway by transforming growth factor-beta. *Methods Mol. Biol*. 142:125–131.
25. Fujita, Y., S. Maruyama, H. Kogo, S. Matsuo, and T. Fujimoto. 2004. Caveolin-1 in mesangial cells suppresses MAP kinase activation and cell proliferation induced by bFGF and PDGF. *Kidney Int*. 66:1794–1804.
26. Wang, X.M., H.P. Kim, R. Song, and A.M. Choi. 2006. Caveolin-1 confers antiinflammatory effects in murine macrophages via the MKK3/p38 MAPK pathway. *Am. J. Respir. Cell Mol. Biol*. 34:434–442.
27. Katzenstein, A.L., and J.L. Myers. 1998. Idiopathic pulmonary fibrosis: clinical relevance of pathologic classification. *Am. J. Respir. Crit. Care Med*. 157:1301–1315.
28. Selman, M., and A. Pardo. 2002. Idiopathic pulmonary fibrosis: an epithelial/fibroblastic cross-talk disorder. *Respir. Res*. 3:3.
29. Yamamoto, Y., T. Kubota, Y. Atoji, and Y. Suzuki. 1996. Structure of the perilobular sheath of the deep proventricular gland of the chicken: presence and possible role of myofibroblasts. *Cell Tissue Res*. 285:109–117.
30. Aono, Y., Y. Nishioka, M. Inayama, M. Ugai, J. Kishi, H. Uehara, K. Izumi, and S. Sone. 2005. *Am. J. Respir. Crit. Care Med*. 171:1279–1285.
31. Schiller, M., D. Javelaud, and A. Mauviel. 2004. TGF-beta-induced SMAD signaling and gene regulation: consequences for extracellular matrix remodeling and wound healing. *J. Dermatol. Sci*. 35:83–92.
32. Sime, P.J., Z. Xing, F.L. Graham, K.G. Csaky, and J. Gauldie. 1997. Adenovector-mediated gene transfer of active transforming growth factor-beta1 induces prolonged severe fibrosis in rat lung. *J. Clin. Invest*. 100:768–776.
33. Raghu, G., W.C. Johnson, D. Lockhart, and Y. Mageto. 1999. Treatment of idiopathic pulmonary fibrosis with a new antifibrotic agent, pirfenidone: results of a prospective, open-label Phase II study. *Am. J. Respir. Crit. Care Med*. 159:1061–1069.
34. Atamas, S.P., I.G. Luzina, J. Choi, N. Tsymbalyuk, N.H. Carbonetti, I.S. Singh, M. Trojanowska, S.A. Jimenez, and B. White. 2003. Pulmonary and activation-regulated chemokine stimulates collagen production in lung fibroblasts. *Am. J. Respir. Cell Mol. Biol*. 29:743–749.
35. Sato, M., D. Shegogue, A. Hatamochi, S. Yamazaki, and M. Trojanowska. 2004. Lysophosphatidic acid inhibits TGF-beta-mediated stimulation of type I collagen mRNA stability via an ERK-dependent pathway in dermal fibroblasts. *Matrix Biol*. 23:353–361.
36. Hocevar, B.A., T.L. Brown, and P.H. Howe. 1999. TGF-beta induces fibronectin synthesis through a c-Jun N-terminal kinase-dependent, Smad4-independent pathway. *EMBO J*. 18:1345–1356.
37. American Thoracic Society. 2002. American Thoracic Society/European Respiratory Society International Multidisciplinary Consensus Classification of the Idiopathic Interstitial Pneumonias. *Am. J. Respir. Crit. Care Med*. 165:277–304.
38. Kuan, C.Y., D.D. Yang, D.R. Samanta Roy, R.J. Davis, P. Rakic, and R.A. Flavell. 1999. The Jnk1 and Jnk2 protein kinases are required for regional specific apoptosis during early brain development. *Neuron*. 22:667–676.
39. Fattman, C.L., L.Y. Chang, T.A. Termin, L. Petersen, J.J. Enghild, and T.D. Oury. 2003. Enhanced bleomycin-induced pulmonary damage in mice lacking extracellular superoxide dismutase. *Free Radic. Biol. Med*. 35:763–771.
40. Tan, R.J., C.L. Fattman, S.C. Watkins, and T.D. Oury. 2004. Redistribution of pulmonary EC-SOD after exposure to asbestos. *J. Appl. Physiol*. 97:2006–2013.
41. Zhou, Z., R. Song, C.L. Fattman, S. Greenhill, S. Alber, T.D. Oury, A.M. Choi, and D. Morse. 2005. Carbon monoxide suppresses bleomycin-induced lung fibrosis. *Am. J. Pathol*. 166:27–37.
42. Cho, K.A., S.J. Ryu, J.S. Park, I.S. Jang, J.S. Ahn, K.T. Kim, and S.C. Park. 2003. Senescent phenotype can be reversed by reduction of caveolin status. *J. Biol. Chem*. 278:27789–27795.
43. Kaminski, N., and N. Friedman. 2002. Practical approaches to analyzing results of microarray experiments. *Am. J. Respir. Cell Mol. Biol*. 27:125–132.
44. Godfrey, T.E., S.H. Kim, M. Chavira, D.W. Ruff, R.S. Warren, J.W. Gray, and R.H. Jensen. 2000. Quantitative mRNA expression analysis from formalin-fixed, paraffin-embedded tissues using 5′ nuclease quantitative reverse transcription-polymerase chain reaction. *J. Mol. Diagn*. 2:84–91.